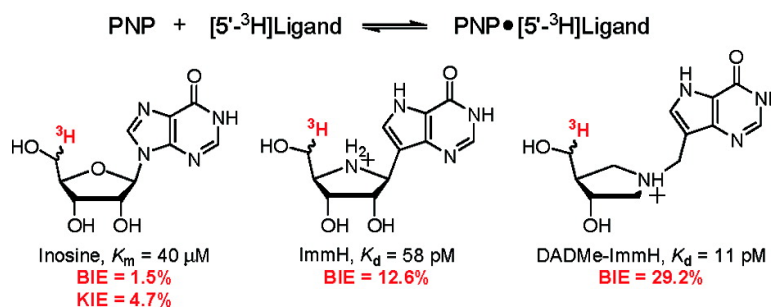


## Transition-State Interactions Revealed in Purine Nucleoside Phosphorylase by Binding Isotope Effects

Andrew S. Murkin, Peter C. Tyler, and Vern L. Schramm

*J. Am. Chem. Soc.*, **2008**, 130 (7), 2166-2167 • DOI: 10.1021/ja7104398

Downloaded from <http://pubs.acs.org> on February 8, 2009



### More About This Article

Additional resources and features associated with this article are available within the HTML version:

- Supporting Information
- Access to high resolution figures
- Links to articles and content related to this article
- Copyright permission to reproduce figures and/or text from this article

[View the Full Text HTML](#)

## Transition-State Interactions Revealed in Purine Nucleoside Phosphorylase by Binding Isotope Effects

Andrew S. Murkin,<sup>†</sup> Peter C. Tyler,<sup>‡</sup> and Vern L. Schramm<sup>\*†</sup>

Department of Biochemistry, Albert Einstein College of Medicine, Bronx, New York, and Carbohydrate Chemistry Team, Industrial Research Ltd., Lower Hutt, New Zealand

Received November 19, 2007; E-mail: vern@aecom.yu.edu

Enzymatic transition-state (TS) analogues capture the lowered activation energy for catalysis as binding energy and TS formation has been explained in both dynamic and thermodynamic terms.<sup>1,2</sup> Thermodynamic interpretation of catalysis and TS analogue binding proposes tight binding of reactants at the TS. This binding is converted directly into binding energy of TS analogues. The dynamic interpretation of catalysis proposes formation of the TS by a coordinated dynamic excursion of the protein that does not require tight binding at the TS.<sup>2</sup> Tight binding of TS analogues in the dynamic model of TS formation involves conversion of the dynamic TS excursion into a static, stable structure organized around the chemically stable TS analogue. Here an experimental test of these hypotheses is achieved for human purine nucleoside phosphorylase (PNP) through a comparison of chemically intrinsic kinetic isotope effects (KIEs) from TS formation<sup>3</sup> and binding isotope effects (BIEs) for TS analogue interactions.<sup>4</sup>

Isotope effects, structural studies, and computational analysis of PNP have established a ribooxacarbenium TS with reaction coordinate motion from His257 causing electron repulsion from the ribosyl oxygen to the hypoxanthine leaving group (Figure 1).<sup>3,5,6</sup> Immobilization of the 5'-hydroxyl group in the Michaelis complex generates a 1.5% BIE from [5'-<sup>3</sup>H]inosine with an additional 4.7% intrinsic chemical KIE arising from TS distortion and electronics. Mutation of His257 alters the kinetics, inhibition, structure, BIEs, and KIEs found with human PNP.<sup>7</sup>

5'-<sup>3</sup>H BIEs and KIEs of inosine with PNP allow distinction between bond vibrational distortions that occur upon binding of the substrate from those distortions that arise from chemistry at the TS. Comparing the [5'-<sup>3</sup>H]inosine isotope effects with those of [5'-<sup>3</sup>H]ImmH and [5'-<sup>3</sup>H]DADMe-ImmH (pM TS analogues) permits direct analysis of the bond distortions experienced at the TS with those that occur on the binding of TS analogues.

While small bond distortional changes result from converting unbound [5'-<sup>3</sup>H]inosine to the Michaelis complex, greater distortional change results from formation of the TS (BIE 1.5% vs KIE 4.7%). If TS analogue binding mimics the distortional geometry of the TS, we might expect TS analogues to show BIEs similar to the combined KIE and BIE found in catalysis (*V*/*K* KIE of ~6%). If the binding of TS analogues converts a dynamic excursion that forms the TS into a collapsed protein conformation, larger BIEs would be expected for TS analogues than for inosine.

ImmH and DADMe-ImmH are potent inhibitory TS analogues of PNP with *K*<sub>d</sub> values of 58 and 11 pM, respectively.<sup>7–9</sup> The *K*<sub>m</sub>/*K*<sub>d</sub> values of 690 000 and 3 700 000 relative to inosine indicate substantial capture of the TS effect (Figure 1). These compounds were synthesized with one of the 5'-hydrogens labeled with <sup>3</sup>H and separately with <sup>14</sup>C as a remote label. Tritium was introduced by reduction of the corresponding 5'-aldehydes with Na[<sup>3</sup>H]BH<sub>4</sub>, giving

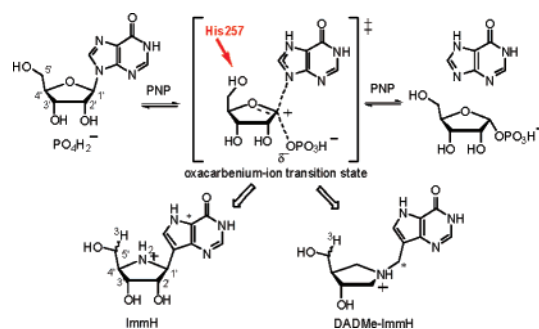


**Figure 1.** Phosphorolysis of inosine catalyzed by PNP. The oxacarbenium ion TS, its chemically stable analogues, ImmH and DADMe-ImmH, and positions of isotopic and remote labels are shown.

mixtures of the 5'-*R* and 5'-*S* monolabeled isomers. <sup>14</sup>C was incorporated into the 9-deazahypoxanthine moiety of ImmH and the methylene bridge of DADMe-ImmH (see Supporting Information).

Competitive binding of [5'-<sup>3</sup>H]ImmH and [5-<sup>14</sup>C]ImmH and of [5'-<sup>3</sup>H]DADMe-ImmH and [methylene-<sup>14</sup>C]DADMe-ImmH was performed using the ultrafiltration method.<sup>10,11</sup> Solutions of 50 mM KPO<sub>4</sub> (pH 7.4), 20–60 μM inhibitor (~4:1 ratio of <sup>3</sup>H:<sup>14</sup>C by dpm) and 10 μM PNP were applied to an ultrafiltration apparatus (quadruplicate 100 μL samples), and 30 psi argon was applied until approximately half of the solution had passed through the dialysis membrane (10 kDa MW retention limit) into the lower well (90–120 min). Samples from both upper and lower wells (30 μL) were mixed with ten mL of scintillation fluid (Perkin-Elmer UltimaGold) and counted for at least six cycles of 10 min each. Spectral deconvolution of <sup>3</sup>H and <sup>14</sup>C was performed as described previously using a <sup>14</sup>C standard in a matrix identical to the BIE samples. The BIEs were calculated according to:

$$\text{BIE} = \frac{{}^{14}\text{C}_T/{}^{14}\text{C}_B - 1}{{}^3\text{H}_T/{}^3\text{H}_B - 1} \quad (1)$$

where <sup>14</sup>C<sub>T</sub> and <sup>14</sup>C<sub>B</sub> are the <sup>14</sup>C counts in the top and bottom wells, respectively, and <sup>3</sup>H<sub>T</sub> and <sup>3</sup>H<sub>B</sub> are the <sup>3</sup>H counts in the top and bottom wells, respectively.

ImmH and DADMe-ImmH yielded large BIEs of 13% and 29%, respectively, which dwarf the 1.5% BIE and the 4.7% KIE measured for the substrate inosine (Table 1).<sup>7</sup> Thus, both TS analogue inhibitors of PNP undergo larger bond vibrational distortions than occur at the TS.

Factors contributing to a 5'-<sup>3</sup>H BIE include the degree of hyperconjugation between the σ\* orbitals of the 5'-C–H bonds and neighboring electron density at C-4' and O-5'. The contribution to the BIE due to C-4' interactions was estimated by model calculations (Gaussian 98, B3LYP/6-31G\*\* theory) comparing free ImmH, with

<sup>†</sup> Albert Einstein College of Medicine.

<sup>‡</sup> Industrial Research, Ltd.

**Table 1.**  $5'$ - $^3\text{H}$  Binding Isotope Effect Data for Human PNP

ligands	$K_i$ or $K_m$	BIE <sup>a</sup>
$[5' \text{-}^3\text{H}]$ -, $[5' \text{-}^{14}\text{C}]$ Ino	40 $\mu\text{M}$	1.015 $\pm$ 0.003 (9) <sup>b</sup>
$[5' \text{-}^3\text{H}]$ -, $[5' \text{-}^{14}\text{C}]$ ImmH	58 pM	1.126 $\pm$ 0.005 (32)
$[5' \text{-}^3\text{H}]$ -, $[^{14}\text{C}]$ DADMe-ImmH	11 pM	1.292 $\pm$ 0.012 (27)

<sup>a</sup> BIE  $\pm$  standard deviation. The number of replicates is given in parentheses. <sup>b</sup> From reference 7.

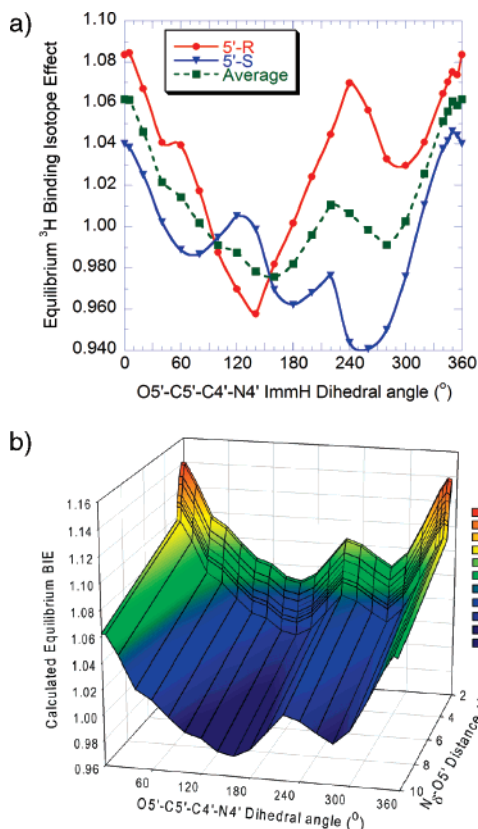


**Figure 2.** Calculated effects of  $5'$ -hydroxyl orientation and polarization on the  $5'$ - $^3\text{H}$  BIE. (a) The  $\text{O}5'-\text{C}5'-\text{C}4'-\text{N}4'$  dihedral angle of “unbound” ImmH models was varied and compared to the “bound” model having dihedral angles fixed to those in the crystal structure, and the corresponding BIEs were calculated using ISOEFF98. Results are shown for the pro-R and pro-S hydrogens, separately and as an equally weighted average. (b) An imidazole molecule was added to the “bound” ImmH model in panel a with fixed orientation as found in the crystal structure, but with  $\text{N}_\delta\text{-O}5'$  distance varying from 2.84 to 2.20 Å. The BIE is the average for  $\text{H}_R$  and  $\text{H}_S$ . The green curve in panel a can be seen as the slice at an  $\text{N}-\text{O}$  distance of 10 Å.

little rotational restriction of the  $5'$ -hydroxyl, to ImmH bound in the active site, which X-ray crystallographic data (PDB ID 1RR6)<sup>7</sup> indicates is fixed with an  $\text{O}5'-\text{C}5'-\text{C}4'-\text{N}4'$  dihedral angle of  $59.3^\circ$  (Figure 2a). Unbound ImmH exists predominantly with a dihedral angle between  $-60^\circ$  and  $+60^\circ$ , predicting a geometric BIE contribution upon binding of 6% or less. In a similar manner, having the  $\text{H}-\text{O}5'-\text{C}5'-\text{C}4'$  torsion angle fixed by H-bonding to His257 could account for an additional 14% of the  $5'$ - $^3\text{H}$  BIE, as has been shown by Lewis and Schramm using an isopropanol–formate model.<sup>11</sup> H-bonding with an enzymatic base also polarizes the  $5'$ -OH, imparting negative charge character on  $\text{O}5'$  and enhancing hyperconjugation, thereby loosening the  $5'$ -C–H bonds. Pairing ImmH with an imidazole molecule having the same geometry as

His257 in the crystal structure ( $\text{N}_\delta\text{-O}5'$  distance = 2.84 Å) elevates the calculated BIEs at all  $5'$ -OH dihedral angles by 4% (Figure 2b). As the base is brought closer, the calculated BIEs increase sharply by as much as 6% at 2.6 Å, which is within error limits of the X-ray structure.

If each of the above factors contributes multiplicatively to the overall BIE, combinations may account for a  $5'$ - $^3\text{H}$  BIE of up to 28% ( $1.06 \times 1.14 \times 1.06$ ), a value close to the observed value of 29.2% for  $[5' \text{-}^3\text{H}]$ DADMe-ImmH. Additional factors that cannot be easily observed and modeled may also contribute to this BIE of unprecedented magnitude. For instance, a  $3^\circ$  distortion of the  $\text{sp}^3$  geometry of C- $5'$  imposed by active site interactions has been shown by Horenstein et al. to account for an observed isotope effect of 5%.<sup>12</sup> Additionally, if the H-bond to the  $5'$ -OH is stronger than in our simplified model, the  $5'$ -C–H bonds would become looser,<sup>13</sup> leading to a larger BIE.

Prior to these studies, the largest BIE reported for any protein–ligand system was 8.5% for  $[4\text{-}^3\text{H}]$ NAD<sup>+</sup> with lactate dehydrogenase.<sup>14</sup> The magnitude of this BIE on the binding of a substrate is remarkable, owing to substantial bond loosening that occurs at the site of hydride acceptance in the cofactor. Interestingly, the association of  $[1\text{-}^{18}\text{O}]$ oxamate to the NADH-bound form of this enzyme resulted in a BIE of  $-1.6\%$ , and this, to our knowledge, was the only previous determination of an IE for the binding of an inhibitor.<sup>15</sup> The large BIEs demonstrated here illustrate substantial bond distortion remote from the site of bond breaking upon binding of TS analogues.

The BIEs for ImmH and DADMe-ImmH increase with the binding affinity (Table 1). Thus, forces at the  $5'$  position increase according to the energy difference between free and bound states. Distortion of  $[5' \text{-}^3\text{H}]$ inosine at the TS and/or combined with the Michaelis complex is small compared to the TS analogues, supporting large bond vibrational distortions of TS analogues but not of inosine at its ribooxacarbenium ion TS.

**Acknowledgment.** This work was supported by NIH Grant GM41916.

**Supporting Information Available:** Synthetic methods for selected compounds, molecular model calculations, and derivation of eq 1. This material is available free of charge via the Internet at <http://pubs.acs.org>.

## References

- Wolfenden, R. *Bioorg. Med. Chem.* **1999**, *7*, 647–652.
- Schramm, V. L. *Arch. Biochem. Biophys.* **2005**, *433*, 13–26.
- Lewandowicz, A.; Schramm, V. L. *Biochemistry* **2004**, *43*, 1458–1468.
- Schramm, V. L. *Curr. Opin. Chem. Biol.* **2007**, *11*, 529–536.
- Fedorov, A.; Shi, W.; Kicska, G.; Fedorov, E.; Tyler, P. C.; Furneaux, R. H.; Hanson, J. C.; Gainsford, G. J.; Lares, J. Z.; Schramm, V. L.; Almo, S. C. *Biochemistry* **2001**, *40*, 853–860.
- Nunez, S.; Antoniou, D.; Schramm, V. L.; Schwartz, S. D. *J. Am. Chem. Soc.* **2004**, *126*, 15720–15729.
- Murkin, A. S.; Birck, M. R.; Rinaldo-Matthis, A.; Shi, W.; Taylor, E. A.; Almo, S. C.; Schramm, V. L. *Biochemistry* **2007**, *46*, 5038–5049.
- Miles, R. W.; Tyler, P. C.; Furneaux, R. H.; Bagdassarian, C. K.; Schramm, V. L. *Biochemistry* **1998**, *37*, 8615–8621.
- Lewandowicz, A.; Tyler, P. C.; Evans, G. B.; Furneaux, R. H.; Schramm, V. L. *J. Biol. Chem.* **2003**, *278*, 31465–31468.
- Schramm, V. L. *J. Biol. Chem.* **1976**, *251*, 3417–3424.
- Lewis, B. E.; Schramm, V. L. *J. Am. Chem. Soc.* **2003**, *125*, 4785–4798.
- Horenstein, B. A.; Parkin, D. W.; Estupinan, B.; Schramm, V. L. *Biochemistry* **1991**, *30*, 10788–10795.
- Maiti, N. C.; Zhu, Y.; Carmichael, I.; Serianni, A. S.; Anderson, V. E. *J. Org. Chem.* **2006**, *71*, 2878–2880.
- LaReau, R. D.; Wan, W.; Anderson, V. E. *Biochemistry* **1989**, *28*, 3619–3624.
- Gawlita, E.; Paneth, P.; Anderson, V. E. *Biochemistry* **1995**, *34*, 6050–6058.

JA7104398